Linear Holding for Reducing Additional Delays Experienced by Flights Subject to Ground Holding at no Extra Fuel Cost

Yan Xu (corresponding author)
Technical University of Catalonia
Office C3-121, Esteve Terradas, 5
Castelldefels 08860, Catalonia, Spain
Email: yan.xu@estudiant.upc.edu

Suwan Yin
College of Civil Aviation
Nanjing University of Aeronautics and Astronautics
NO.29 Jiangjun Road, Nanjing City, China
Email: suwan.yin@nuaa.edu.cn

Ramon Dalmau
Technical University of Catalonia
Office C3-121, Esteve Terradas, 5
Castelldefels 08860, Catalonia, Spain
Email: ramon.dalmau@upc.edu

Dr. Xavier Prats
Department of Telecommunications and Aerospace Engineering
Technical University of Catalonia
Office C3-104, Esteve Terradas, 5
Castelldefels 08860, Catalonia, Spain
Email: xavier.prats@upc.edu

Dr. Ke Han
Centre for Transport Studies
Department of Civil and Environmental Engineering
Imperial College London
South Kensington Campus, Skempton Building
SW7 2AZ London, United Kingdom
Email: k.han@imperial.ac.uk

Submitted for presentation and publication to the
96th Annual Meeting of the Transportation Research Board
January 8 - 12, 2017

July 31, 2016

$7,450\ words\ [4,450\ words + 11\ figures \times 250 + 1\ table \times 250]$

ABSTRACT
This paper presents a method to implement linear holding (LH) for flights subject to ground holding in context of the upcoming Trajectory Based Operations in air transportation, aimed at reducing additional delays raised from the lack of coordination between various traffic management initiatives (TMIs) without incurring extra fuel consumption. Firstly, motivated from previous works on the features of LH to absorb delays airborne, a potential applicability of LH to compensate part of the fixed ground holding is proposed. Then, the dynamic adjustment of LH in response to TMIs-associated tactical delays is formulated as a multi-stage aircraft trajectory optimization problem, addressing both pre- and post-departure additional delays. Finally, the effects of performing LH are investigated for a particular flight, discussing the changes of vertical trajectory, speed profile, fuel consumption and flight timeline, for each step of optimization. Results suggest that additional delays of 25mins in a typical case study can be totally recovered at no extra fuel cost. A notable extent of delay reduction observed from the simulation assessment further supports the benefits of LH for reducing different combinations of additional delays.

INTRODUCTION

In the recent 16th ATIO (AIAA) conference*, Bilimoria (1) presented an analysis of the additional delays experienced by flights subject to ground holding for Ground Delay Programs (GDPs) or Airspace Flow Programs (AFPs), with statistic results obtained from five airports of arrivals suffering the most pre-departure ground holding in 2015, suggesting the additional delays of those EDCT (Expect Departure Clearance Time) affected flights were substantially larger in four of the five airports (about two to three times on average) than for arrivals that were not subject to ground holding. At the same conference, a similar analysis of "double delay" (or "double penalty"), due to the interaction between GDPs and arrival metering (terminal scheduling delays), was presented by Evans and Lee (2), providing a deep dive into the underlying causes of those double delays and the circumstances in which they occur in real operations.

Imagine a flight may be held on the ground through a GDP/AFP, before being rerouted around a thunderstorm, and then subject to Miles in Trail (MIT) as it passes through a congested sector, as described in (3). The joint impact of all these initiatives together may not be well coordinated, and there may be perceived inequities in their implementation, which in turn yields the possibility that unnecessary delay may have been performed by means of ground holding (currently the assigned GDP/AFP delay is entirely transferred from the capacity affected area to departure airport while imposed on EDCT) before encountering other initiatives generating delays as well, and thus again pushes back its final arrival time.

The above discussions all point to a drawback of ground holding, the low flexibility, especially in terms of integrating among various Traffic Management Initiatives (TMIs), as indicated prior in (4, 5) as a real problem in National Airspace System. Even so, ground holding is still preferred nowadays to absorb delays because less fuel consumption is incurred if compared with typical airborne holding. However, in previous works (6, 7, 8), a cruise speed reduction strategy was introduced aimed at partially absorbing delays airborne, where ground delayed flights were allowed to cruise at the lowest possible speed in such a way the specific range (i.e., the distance flown per unit of fuel) remained the same. In this situation, the fuel consumption kept unchanged while some linear holding (LH) was performed in compensation with the reduced ground holding. More recently, this strategy was further extended in (9) by using trajectory optimization techniques, where the whole flight profile including climb, cruise and descent phases was subject of optimization, being a remarkable increase reported on the maximum amount of LH that can be done without extra fuel consumption.

With the paradigm shift of an airspace-based Air Traffic Management (ATM) to the Trajectory Based Operation (TBO), the proposed LH could provide a high flexibility in cost-based delay management. Therefore, the purpose of this paper is to implement LH to substitute part of the ground holding, adjusted dynamically in response to potential TMIs that may produce tactical delays during pre- and post-departure phases, in such a way to reduce the additional delays as much as possible at no extra fuel cost. For this purpose, an optimal trajectory generation technique is used to formulate each of the steps of the implementation, followed by a case study illustrating in detail the effects of dynamic adjustment of LH to a specific flight, as well as a simulation assessment on the capability of delay recovery with respect to different TMIs-associated delay combinations.

*16th AIAA Aviation Technology, Integration, and Operations Conference, 13-17 June 2016, Washington, D.C.

MOTIVATION

Fig. 1 illustrates some key flight-related events (blue rectangles) and time intervals. According to (1), each of these events is associated with a possible additional delay (red rectangles) as has been examined for the variance between its scheduled time and actual time, utilizing historical flight operations data from five airports (LGA, SFO, EWR, JFK, PHL) whose arrivals experienced the most pre-departure ground holding in 2015.

Consider a particular flight is filed into a GDP (much like an AFP but the latter is for specifically en route capacity reduction), with its scheduled arrival time captured and thus postponed by a certain GDP delay, i.e., from “Scheduled Flight” to “Scheduled Flight in GDP” in Fig. 1. Currently, the assigned delay is entirely transferred from arrival to departure airport in the form of ground holding (GH) to avoid relative costly airborne holding, and to obtain a parallel shift on the scheduled arrival time (Wheels On). However, due to the possible additional delays, the already delayed time of Wheels On could be delayed again, as from “Scheduled Flight in GDP” to “Actual Flight in GDP”. In such situation, extra fuel has to be consumed from increasing flight speed if any delay recovery is required.

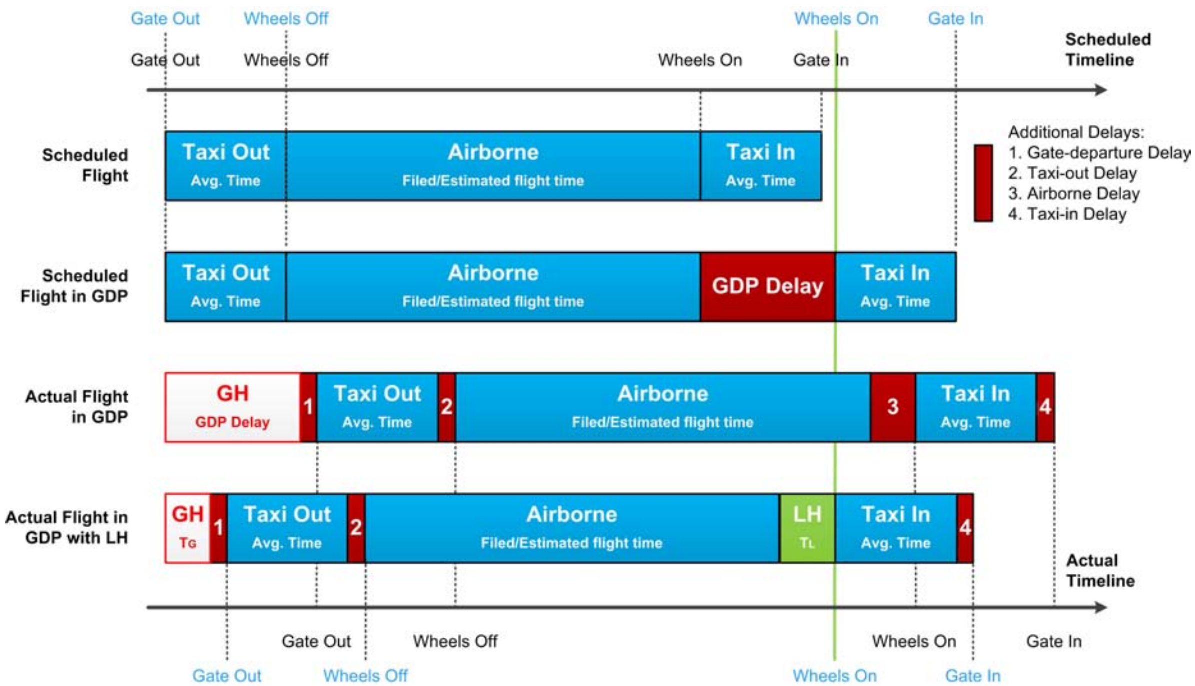

FIGURE 1 Schematic of additional delays subject to a GDP scenario and the corresponding applicability of LH.

Then, for “Actual Flight in GDP with LH” in Fig. 1, the ground holding is shortened because part of the assigned delay is absorbed by LH airborne, while still meeting the scheduled arrival time in GDP (green line). Thanks to the flexibility of LH, every time an additional delay is encountered during the execution of the flight, the required LH can be updated through speed control, which, based on a concept of equivalent speed, may yield no extra fuel consumption.

The equivalent speed has been introduced in (9), as shown in Fig. 2, from which it can be noticed that within the intervals between the nominal speed (V^i_{nom}) and equivalent speed (V^i_{eq}) with

i for climb, cruise and descent flight phases, the amount of fuel consumption (or specific range) will not exceed the nominal one, and LH can be realized by speed reduction from nominal speed.

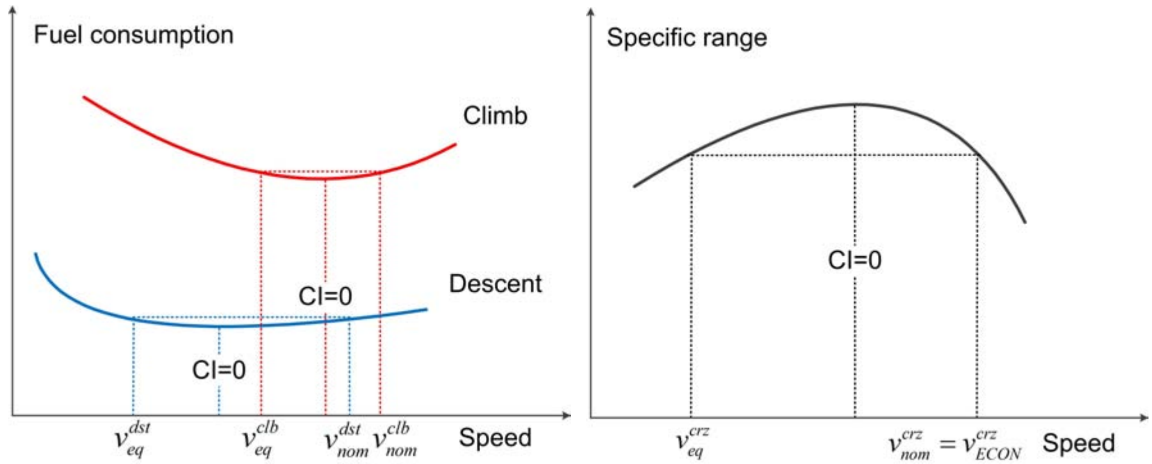

(a) Climb and Descent (b) Cruise

FIGURE 2 The equivalent speeds in climb, descent and cruise phases.

In this paper, the initially scheduled flight is regarded as nominal flight. Since airline operators also consider time-related costs (e.g., guarantee connecting passengers, flight crew payments) when planning their flights, higher speeds are usually preferred despite the associated extra fuel, while this preference is typically realized by Cost Index (CI), a feature of current on-board Flight Management System (FMS), that represents the ratio between time-based cost and the cost of fuel (10). The higher the CI is, the more importance will be given to flight time and the faster the scheduled flight speed will be.

Nonetheless, the speed intervals (between the nominal and equivalent speed) as well depend on the function curves of fuel consumption (or specific range), as shown in Fig. 2, which in turn are aircraft performance, atmospheric magnitudes and flight status dependent, and should change continuously along with the process of a particular flight. Hence, a continuous optimal control problem will be discussed below to formulate the aforementioned implementation of LH as a 4D trajectory optimization.

OPTIMAL TRAJECTORY GENERATION

The optimization of aircraft trajectory requires the definition of a mathematical model representing aircraft dynamics and performances, along with a model for certain atmospheric criteria. In this paper, a point-mass dynamics model, an enhanced performance model using manufacturer performance data and the International Standard Atmosphere (ISA) have been considered. For more details, the readers may refer to (11).

Scheduled trajectory filed into a GDP with an EDCT assigned

Following the conventional operation concept, a generic aircraft trajectory can be divided into several segments $i \in [1, \ldots, N]$. For each segment defined over the time window $[t_0^{(i)}, t_f^{(i)}]$ the state vector $x^{(i)} = [v \; s \; h \; m]^T$ is composed by the true airspeed (TAS), along path distance, altitude and mass of the aircraft, respectively; the control vector $u^{(i)} = [T \; \gamma]$ includes the aircraft thrust and flight path angle (11); and a parameter $p^{(i)}$ vector of variables that are not time depended is also defined.

For the initially scheduled flight, the objective of trajectory optimization is to minimize a compound cost function J over the whole time window $[t_0^{(1)}, t_f^{(N)}]$ as follows:

$$J = \int_{t_0^{(1)}}^{t_f^{(N)}} (FF(t) + CI)dt \tag{1}$$

where $FF(t)$ is the fuel flow and CI the Cost Index, combined as to reflect the direct operating costs (10).

The constraints come from different aspects, while the first of particular important is the dynamics of the system (point-mass dynamics model). Then, some algebraic event constraints fixing the initial $x(t_0^{(1)})$ and final $x(t_f^{(N)})$ state vector must be satisfied. In this paper, the initial and final points are taken, respectively, at the moment the slats are retracted (after taking off) and extended (before landing). The remaining parts of take-off and approaching are not optimized due to the heavy constraints from operational procedures.

Some bounds (known as box constraints) on the control variables are specified as follows:

$$\gamma_{min} \leq \gamma \leq \gamma_{max} \tag{2}$$

where γ_{min} and γ_{max} are aircraft dependent scalars. However, the maximum T_{max} and minimum T_{min} thrust are not scalars but functions of the state variables. Therefore, this control is bounded by additional path constraints:

$$T_{min} \leq T \leq T_{max} \tag{3}$$

Similarly, box constraints for the state variables are not required, since they are bounded by generic path constraints on auxiliary variables such as the Mach number (M) and the Calibrated Airspeed (CAS, V_{CAS}):

$$M_{GD} \leq M \leq MMO; \; V_{GD} \leq V_{CAS} \leq VMO \tag{4}$$

where MMO and VMO are the maximum operational Mach and CAS, respectively, and M_{GD} and V_{GD} are green dot speeds (12), which approximate the best lift to drag ratio speed in clean configuration.

In order to ensure the continuity of the trajectory composed by different segments, link constraints must be defined at the final point and initial point of each segment, on all the state variables:

$$x^{(i)}(t_f^{(i)}) = x^{(i+1)}(t_0^{(i+1)}); \; i = 1, ..., N-1 \tag{5}$$

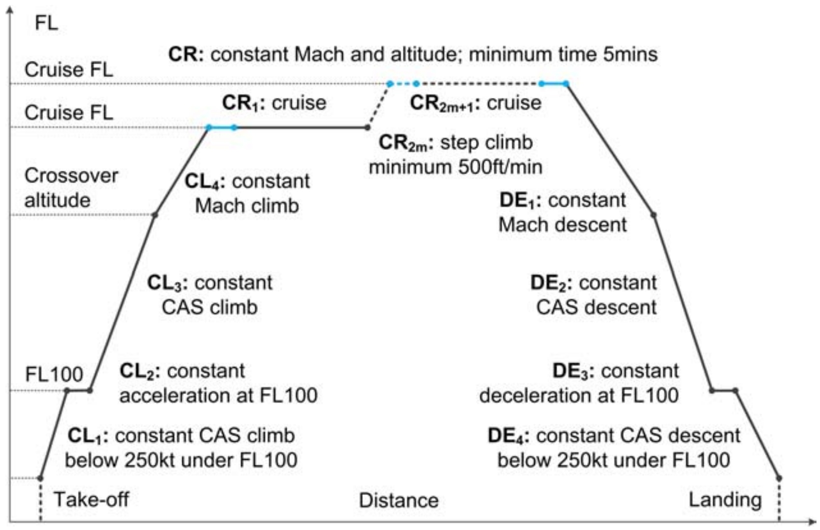

FIGURE 3 Flight profile constraints in accordance with typical ATM with respect to subdivided segments.

Next, additional path and event constraints of the conventional flight profile which are flight segment dependent must be considered, to guarantee the optimized trajectory be consistent with typical ATM operations and regulations. These constraints are summarized in Fig. 3.

It should be noted that in front of each cruise flight level, a short cruise segment less than 1min is attached allowing speed adjustment, and so does the end of the last cruise phase, as shown with the blue ones in Fig. 3, in such a way that the excessive influences from the link constraints (Eq. 5) can be avoided when implementing LH. More mathematical details on the formulation of this flight profile can be found in (11).

In addition to the flight profile, a flight route must be defined either in terms of Great Circle Distance (GCD) between city-pair airports, or by using ATM service route waypoints and published procedures (such as standard instrumental departures and arrivals).

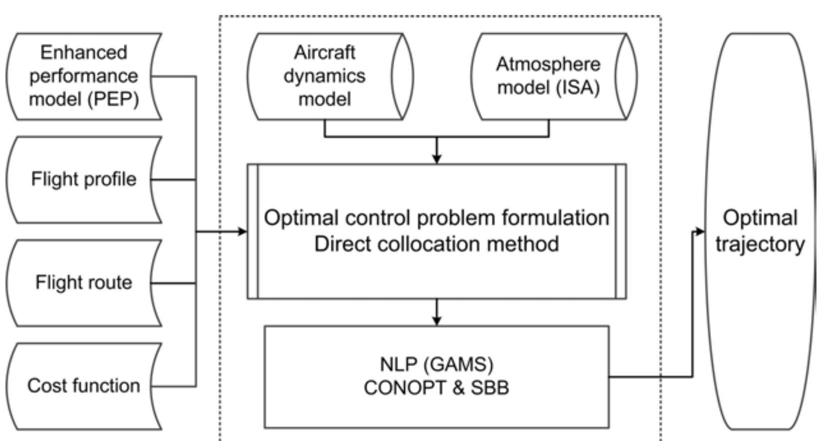

FIGURE 4 The main process in generating the optimal aircraft trajectory.

To find the optimal solution of the formulated optimal control problem, direct collocation methods (13) are used in this paper, which discretize the time histories of control and state variable at a set of nodal or collocation points, transforming the original continuous (infinite) optimal control problem into a (discrete and finite) nonlinear programming (NLP) optimization problem. The new finite variable NLP problem is solved by using solvers CONOPT (as NLP) and SBB as MINLP (mixed integer nonlinear programming), both bundled into the GAMS software suite. The whole process is briefly presented in Fig. 4.

Finally, as stated in Sec. 2, the difference between nominal flight and the one performing entirely ground holding lies only on the timeline, maintaining the other 3D trajectory unchanged. Therefore, a parallel movement, being the assigned GDP delay added on EDCT, has to be imposed, when it comes to the situation where ground holding is wholly enforced.

Scheduled trajectory with LH meeting GDP delay at final arrival

For the scheduled flight having LH as another option, the objective function is switched from Eq. 1 to minimize ground holding as presented in Eq. 6, in order to leave enough time to neutralize possible additional delays before departure, where $t_{0(nom)}^{(1)}$ is the initial time of nominal flight,

$$J = t_0^{(1)} - t_{0(nom)}^{(1)} \tag{6}$$

whilst subject to the same constraints in generating nominal trajectory listed in Sec. 3.1, along with below:

$$t_0^{(1)} - t_{0(nom)}^{(1)} \geq 0 \tag{7}$$

$$t_f^{(N)} = t_{f(nom)}^{(N)} + \Delta t_{GDP} \tag{8}$$

$$\int_{t_0^{(1)}}^{t_f^{(N)}} FF(t)dt \leq m(t_{0(nom)}^{(1)}) - m(t_{f(nom)}^{(N)}) \tag{9}$$

Eq. 7 ensures the departure time not earlier than that initially scheduled (i.e., $t_{0(nom)}^{(1)}$). Eq. 8 specifies that the assigned GDP delay Δt_{GDP} is fully experienced at final arrival. Eq. 9 imposes the maximum fuel consumption allowed which equals to the amount consumed by the nominal flight, where $m(t_{0(nom)}^{(1)})$ and $m(t_{f(nom)}^{(N)})$ are respectively the initial and final mass of aircraft, whose difference is the fuel burned on trip.

In this case, the ideal scheduled trajectory performing LH will be generated. If none of the additional delay occurs later, the flight will endure less ground holding but still meet the same arrival slot at the GDP airport as performing entire ground holding, while consuming no extra fuel.

Actual trajectory after pre-departure additional delays experienced

After ready for gate-out, assume an additional delay Δt_1 arises in the gate-departure process (see Fig. 1), followed by another one Δt_2 during taxi-out phase before departure. It should be noted that these delays can be negative, and an airborne holding may be needed if the scheduled LH has reached its maximum (on condition of no extra fuel cost). However, considering the same situation applies in context of only ground holding, these negative delays are out of the scope of this paper and are left for future work.

Then, the ideal scheduled trajectory has to be updated, after experiencing certain additional delays, with the objective function changed to minimizing Eq. 10, i.e., earliest arrival time, where $t^{(N)}_{f(LH)}$ is the final time of the ideal scheduled trajectory with LH,

$$J = t^{(N)}_{f} - t^{(N)}_{f(LH)} \tag{10}$$

The same constraints for the nominal flight and Eq. 9 apply in such situation, but additional constraints are defined to particularize this concept of operation:

$$t^{(N)}_{f} - t^{(N)}_{f(LH)} \geq 0 \tag{11}$$

$$t^{(1)}_{0} = t^{(1)}_{0(LH)} + \Delta t_1 + \Delta t_2 \tag{12}$$

Eq. 11 ensures the final arrival time not earlier than the assigned slot at GDP airport, which is $t^{(N)}_{f(nom)} + \Delta t_{GDP}$, as stated in Eq. 8. Eq. 12 updates the departure time with regards to the amount of additional delays experienced on ground.

Actual trajectory after post-departure additional delays experienced

When airborne, additional delay Δt_3 may arise (see Fig. 1), due to TMIs such as speed instructions to meet MIT restrictions, path stretching (maneuvers) for separating, and race track holding to tactically absorb large delays. The effects from each of them to aircraft trajectory may vary substantially, and because flights are typically under heavy constraints from these TMIs, there is rarely any space for trajectory optimization.

Accordingly, the short flight segment during this phase is regarded as a black box in this paper, being only time and mass (fuel) discretized by fixed values, while keeping other variables continuous and unchanged.

In this case, the objective function is still as presented in Eq. 10, but the initial point of optimization range should move from "slats retracted" to the phase where airborne delay occurs (i.e., initial time is defined as $t^{(1)}_{AD}$). In addition, the flown trajectory must be wholly fixed, along with added constraints below:

$$t^{(1)}_{AD} = t^{(1)}_{AD(LHpre)} + \Delta t_3 \tag{13}$$

$$m(t^{(1)}_{AD}) - m(t^{(1)}_{AD(LHpre)}) = -FF(t^{(1)}_{AD(LHpre)})\Delta t_3 \tag{14}$$

$$\int_{t_{AD}^{(1)}}^{t_f^{(N)}} FF(t)dt \leq m(t_{AD(LHpre)}^{(1)}) - m(t_{f(nom)}^{(N)}) \tag{15}$$

where $t_{AD(LHpre)}^{(1)}$ denotes the time when airborne delay starts. Eq. 13 updates the initial time of optimization with the airborne delay added. Eq. 14 deducts the fuel consumed by using current fuel flow multiplied by delayed time, while Eq. 15 specifies that this part of fuel caused from airborne delay is not taken account into the criteria that no extra fuel is allowed.

NUMERICAL RESULTS

Results have been obtained from a specific case study, where a scheduled flight, from ATL (Atlanta) to LGA (LaGuardia) airport with a GCD of 662nm, is captured in a GDP list issued from LGA and assigned a delay of 40mins. Airbus A320-211, a common two-engine (CFM56-5A1), narrow-body transport aircraft, is arranged to carry out this flight, which takes a typical factor of 81% (6) of its maximum payload (19ton), and selects initially a CI of 30 kg/min in the FMS.

Some assumptions have been taken: 1) each type of additional delay, is set as a fixed number according to the average statistic value from (1), i.e., gate-departure: 9mins, taxi-out: 9mins, airborne: 7mins; 2) airborne delay occurs at the middle of the flight distance, and ends at the same place; 3) no wind conditions are considered; 4) alternate and reserve fuel are not included; 5) only even flight levels are used (FL260 as the lowest altitude); and 6) cruise step climbs are allowed (if any) with 2000ft steps.

In accordance with the flight process, as discussed in Sec. 3, the simulation has been conducted in five steps:

- Step0 (nom): Initially scheduled flight minimizing direct operating costs;
- Step1: Scheduled trajectory filed into a GDP with an EDCT assigned;
- Step2: Scheduled trajectory with LH meeting GDP delay at final arrival;
- Step3: Actual trajectory after pre-departure additional delays experienced; and
- Step4: Actual trajectory after post-departure additional delays experienced.

TABLE 1 Summarized key parameters with respect to different flight phases.

Cases	ATL	Climb				Criuse					Descent				LGA	Total	
	Slot (hh:mm:ss)	Dist (nm)	Speed (kt/kt/M)	Time (min)	Fuel (kg)	AD Slot (hh:mm:ss)	Dist (nm)	Speed (M)	Time (min)	Fuel (kg)	Dist (nm)	Speed (kt/kt/M)	Time (min)	Fuel (kg)	Slot (hh:mm:ss)	Fuel (kg)	Time (min)
nom	**00:00:00**	162.2	250/288/0.77	25.2	1786	**00:47:56**	372.4	0.78	49.9	1831	127.7	0.77/286/250	22.4	327	**01:37:28**	*3945*	*97.5*
Step1	**00:40:00**	162.2	250/288/0.77	25.2	1786	**01:27:56**	372.4	0.78	49.9	1831	127.7	0.77/286/250	22.4	327	**02:17:28**	*3945*	*97.5*
Step2	**00:12:53**	112.7	250/259/0.68	19.9	1467	**00:59:24**	434.2	0.67	77.3	2205	115.4	0.62/201/201	27.3	273	**02:17:28**	*3945*	*124.6*
Step3	**00:30:53**	161.2	250/261/0.74	26.4	1751	**01:21:26**	368.6	0.74	52.0	1779	132.4	0.69/214/225	28.2	310	**02:17:28**	*3840*	*106.6*
Step4	**00:30:53**	161.2	250/261/0.74	26.4	1751	**01:28:26**	379.6	0.74/0.78	52.4	1867	121.4	0.77/306/250	20.8	320	**02:17:28**	*3938*	*99.6*

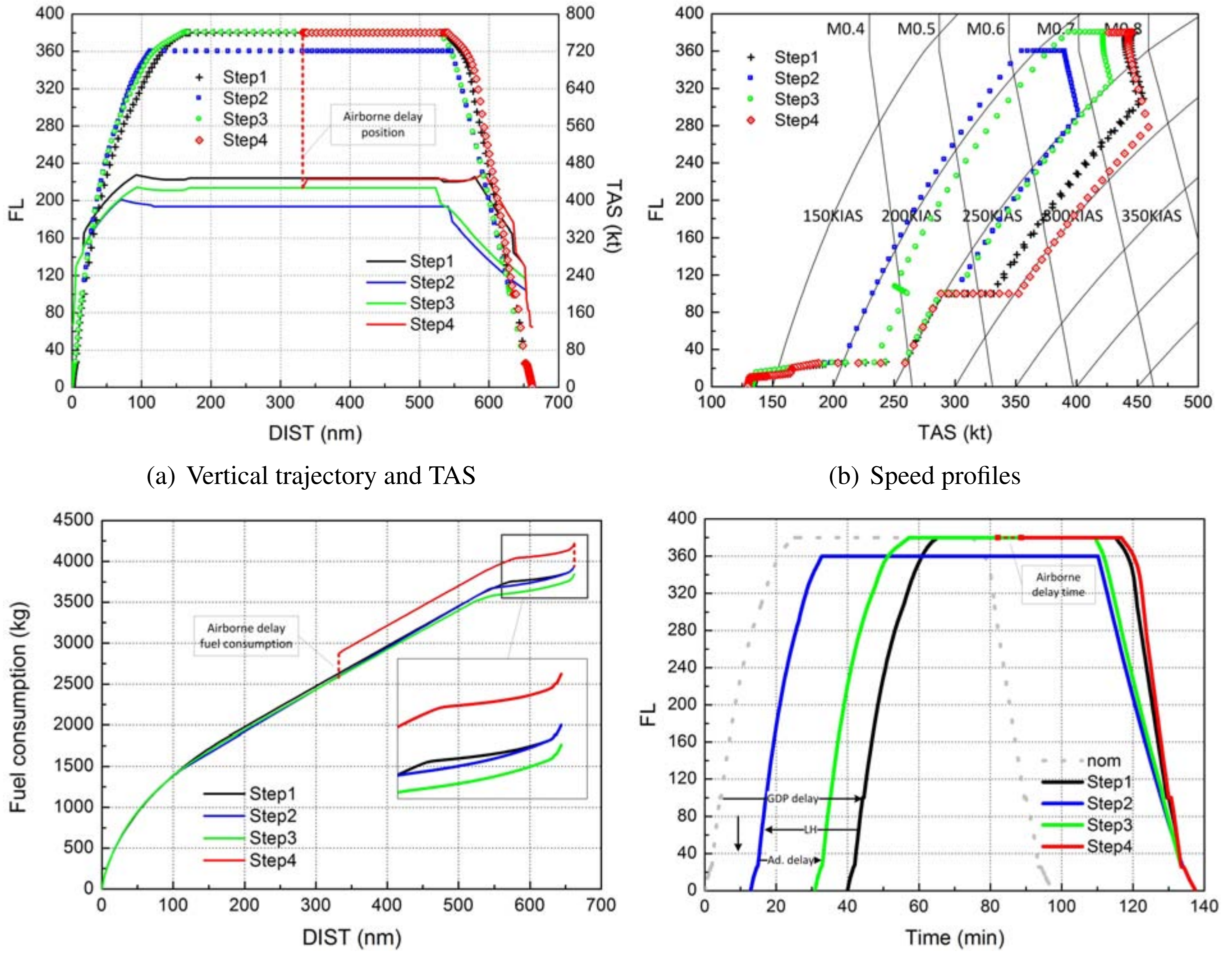

(a) Vertical trajectory and TAS

(b) Speed profiles

(c) Fuel consumption

(d) Vertical trajectory vs. flight time

FIGURE 5 Effects of LH to a specific flight for each of the Step of the study.

Fig. 5(a) plots the vertical trajectory and TAS versus flight distance for each Step. It can be observed that in order to realize the maximum LH, the NLP solver selects a lower cruise flight level (FL) than the nominal (from FL380 to FL360). In general, as the cruise speed reduces (to perform LH, see TAS of Step2), the optimal flight level decreases, to achieve a higher specific range (lower fuel consumption). However, when pre-departure additional delays experienced, the required LH is neutralized from the maximum, leading less speed reduction (see TAS of Step3), and due to the discrete FL (2000ft, one-way), the actual trajectory has to remain its initial altitude (FL380).

With regards to climb and descent phases, the lower the speed is, the steeper the climb and the flatter the descent will be, as can be noticed in Fig. 5(a). However, climb and descent speeds are not continuous in TAS (see Sec. 3). Instead, they are performed mainly from a continuous ac/deceleration process at low altitude, a constant CAS climb/descent, followed by a constant Mach climb/descent over the cross altitude, as shown in Fig. 5(b), with the opposite order for climb and descent (see Speed in Table. 1).

Through an airborne delay, the required LH continues to decline, with a speed increase observed (see TAS of Step4) compared to Step3 for the rest of the trajectory, which is even higher than the nominal, as revealed also in Fig. 5(b), 305kt than 286kt in constant CAS descent. Nevertheless, recall that in Sec. 2 we emphasize that within the interval between the nominal speed and equivalent speed, no extra fuel is needed (see Fig. 2), and in Step4, the descent speed seems out of this interval, while not burning extra fuel, as shown with 3938kg in Table. 1. This is because before the airborne delay, some fuel has been saved in Step3, and if nothing happens the total fuel consumption will be lower than initially scheduled (see Fig. 5(c)), such that it is feasible to have this part of saved fuel consumed for the rest of the flight to maintain a higher speed.

Fig. 5(d) illustrates the changes on flight timeline for the different optimization steps, where we can first tell a parallel shift from nom to Step1 with a length of GDP delay (40mins). It can be also observed that Step2 departs 27mins earlier than Step1 (maximum LH) whilst keeping the same arrival time (i.e., the total flight time is extended by 27mins). However, the total flight time shrinks in Step3 due to the additional pre-departure delays (18mins). Finally, after an airborne delay lasting 7mins (see Step4 in Table. 1), the arrival time still remains the same. That is to say, the additional delays (25mins in total) in this case study are entirely recovered at final arrival (at no extra fuel cost).

In order to see how much delay recovery can be realized when having different combinations of pre- and post-departure delays, more simulations have been performed in the same scenario, changing the value for each delay. Results are as shown in Fig. 6.

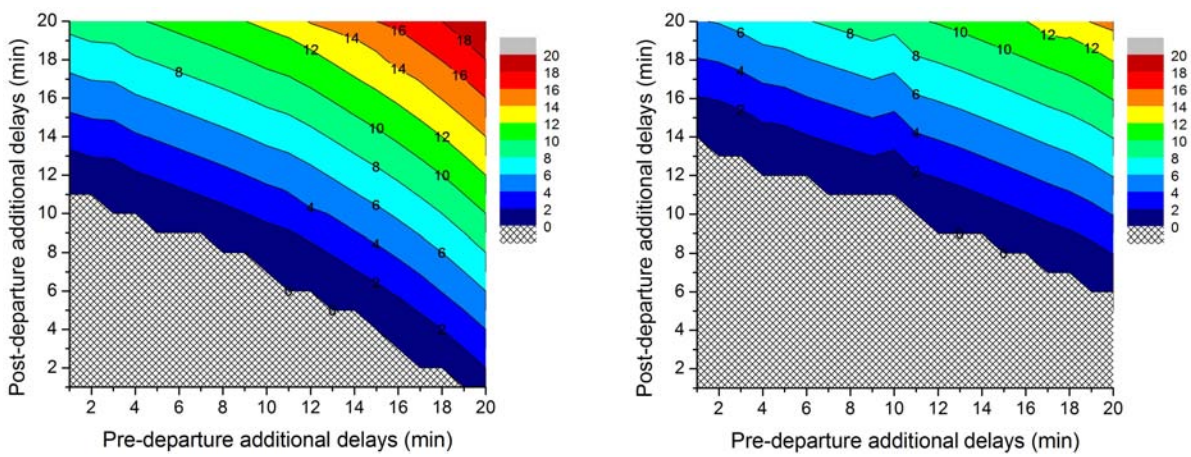

(a) GDP delay of 20 minutes (b) GDP delay of 40 minutes

FIGURE 6 Extent of delay recovery with regards to pre- and post-departure additional delays for GDP delay of 20mins and 40mins respectively.

Two lengths of GDP delay are considered, 20mins and 40mins, where the former is lower than the maximum LH (27mins) of this particular flight, while the latter higher. Fig. 6 shows the actual additional delays endured at final arrival as a function of pre- and post-departure delays, both of which range from 0 to 20mins with a step of 1min. Each colour stripe represents an interval in 2mins, and a blank area highlights where no additional delay is realized.

For the GDP delay of 20mins, since the updated departure time cannot be prior to initially scheduled (see Eq. 7), which restrains the effect of an earlier departure time (Step2) enabled by LH to neutralize additional delays, we can see the delay recovery is limited to some extent compared with that in GDP delay of 40mins (compare Fig. 6(a) and 6(b)).

In both of the cases, it seems that more delay recovery can be yielded with respect to pre-departure than post-departure delays, because there is obviously more space and time for LH (to adjust speed) during the whole flight, rather than partially after airborne delays. For the same reason, the contour lines turn to be flatter in areas where high post-departure and low pre-departure delays occur, if compared to the opposite areas within the same stripe of additional delays.

Finally, worth noting some bumps of the contour line where the pre-departure delay equals to 3mins and 10mins in Fig. 6(a) and 6(b), respectively. Recall again the trade-offs between fuel consumption and flight time shown in Fig. 2. Any LH lower than the maximum contributes to saving some fuel. Therefore, when a specific LH is performed at the same time having the minimum fuel consumed, the saved fuel can be burned at the most to increase flight speed after airborne delays, in such a way to trade for a relative higher delay recovery.

CONCLUSIONS

This paper focused on a problem recently drawing a growing body of research in air transportation, which was mainly about the additional delays experienced by flights subject to ground holding. Inspired from previous works on LH for airborne delay absorption, its potential applicability was proposed to reduce these additional delays at no extra fuel cost. Through multiple stages of optimal trajectory generation, LH was enabled to be implemented along the whole flight phases, and adjusted flexibly in response to different kinds of TMIs and the amounts of additional delays they produce.

While LH proved to be efficient in delay recovery, as results suggested, one precondition must be notified that is an enforced arrival time with full assigned delay imposed, as emphasized in context of TBO. Otherwise, without a full-sized ground holding, airlines may be prone to play tricks on their assigned delays and try to arrive earlier to compete for the reduced available slots, somehow aggravating traffic congestions, as has been defined in (2) as one of the main contributors to double delays.

Future work will aim at the simulation in realistic scenarios. Since the GDP/AFP is typically issued under severe weather conditions, the wind and non-standard atmospheres (which always have great effects on real flights) should be taken into consideration. In addition, after suffering quite a long delay, the operator may be inclined to burn extra fuel than initially scheduled to expect more delay recovered. Thus, further defining a relation between the amount of extra fuel and the extent of delay recovery would be helpful for airlines in decision making.

ACKNOWLEDGMENT

The authors would like to thank Airbus Industrie for the use of PEP (Performance Engineers Program) suite, which allowed us to undertake realistic aircraft performances simulations. This research is partially supported by grants from the Funds of China Scholarship Council (201506830050).

REFERENCES

[1] Bilimoria, K., Analysis of Additional Delays Experienced by Flights Subject to Ground Holding. In *16th AIAA Aviation Technology, Integration, and Operations Conference*, 2016.

[2] Evans, A. D. and P. U. Lee, Analyzing Double Delays at Newark Liberty International Airport. In *16th AIAA Aviation Technology, Integration, and Operations Conference*, 2016.

[3] Dwyer, M., L. Epstein, A. Futer, M. Hogan, K. Howard, R. Oisen, and B. Sharick, *Interactions of Multiple Traffic Management Initiatives: An Initial Analysis, Version 2*, 2011.

[4] Grabbe, S., B. Sridhar, A. Mukherjee, and A. Morando, Traffic Management Advisor Flow Programs: an Atlanta Case Study. In *AIAA Guidance, Navigation, and Control Conference*, 2011, pp. 8–11.

[5] Rebollo, J. and C. Brinton, Brownian Motion Delay Model for the Integration of Multiple Traffic Management Initiatives. In *11th USA/Europe Air Traffic Management Research and Development Seminar (ATM2015)*, 2015.

[6] Delgado, L., X. Prats, and B. Sridhar, Cruise speed reduction for ground delay programs: A case study for San Francisco International Airport arrivals. *Transportation Research Part C: Emerging Technologies*, Vol. 36, 2013, pp. 83–96.

[7] Delgado, L. and X. Prats, Effect of wind on operating-cost-based cruise speed reduction for delay absorption. *IEEE Transactions on Intelligent Transportation Systems*, Vol. 14, No. 2, 2013, pp. 918–927.

[8] Delgado, L. and X. Prats, Operating cost based cruise speed reduction for ground delay programs: Effect of scope length. *Transportation Research Part C: Emerging Technologies*, Vol. 48, 2014, pp. 437–452.

[9] Xu, Y., R. Dalmau, and X. Prats, Effects of speed reduction in climb, cruise and descent phases to generate linear holding at no extra fuel cost. In *7th International Conference on Research in Air Transportation (ICRAT)*, 2016.

[10] Airbus, *Getting to grips with the cost index, Issue II. Flight Operations Support and Line Assistance (STL), Customer Services Directorate. Blagnac*, 1998.

[11] Dalmau, R. and X. Prats, Fuel and time savings by flying continuous cruise climbs: Estimating the benefit pools for maximum range operations. *Transportation Research Part D: Transport and Environment*, Vol. 35, 2015, pp. 62–71.

[12] Airbus, *Flight Crew Operation Manual (FCOM). A320. Version 1.3.1*, 1993.

[13] Betts, J. T., Survey of numerical methods for trajectory optimization. *Journal of guidance, control, and dynamics*, Vol. 21, No. 2, 1998, pp. 193–207.